Developmental Biology 397 (2015) 151–161

Contents lists available at ScienceDirect

Developmental Biology

journal homepage: www.elsevier.com/locate/developmentalbiology

The BED finger domain protein MIG-39 halts migration of distal tip cells in *Caenorhabditis elegans*

Tetsuhiro Kikuchi [a], Yukimasa Shibata [a], Hon-Song Kim [a], Yukihiko Kubota [a,b], Sawako Yoshina [c], Shohei Mitani [c], Kiyoji Nishiwaki [a,*]

[a] Department of Bioscience, Kwansei Gakuin University, 2-1 Gakuen, Sanda 669-1337, Japan
[b] Department of Developmental Biology and Neurosciences, Graduate School of Life Sciences, Tohoku University, 2-1-1 Katahira, Aoba-ku, Sendai 980-8577, Japan
[c] Department of Physiology, Tokyo Women's Medical University School of Medicine, Tokyo 162-8666, Japan

ARTICLE INFO

Article history:
Received 6 June 2014
Received in revised form
8 October 2014
Accepted 14 October 2014
Available online 31 October 2014

Keywords:
BED-finger domain
Rac GTPase
Cell migration
Epithelial tube morphogenesis

ABSTRACT

Organs are often formed by the extension and branching of epithelial tubes. An appropriate termination of epithelial tube extension is important for generating organs of the proper size and morphology. However, the mechanism by which epithelial tubes terminate their extension is mostly unknown. Here we show that the BED-finger domain protein MIG-39 acts to stop epithelial tube extension in *Caenorhabditis elegans*. The gonadal leader cells, called distal tip cells (DTCs), migrate in a U-shaped pattern during larval development and stop migrating at the young adult stage, generating a gonad with anterior and posterior U-shaped arms. In *mig*-39 mutants, however, DTCs overshot their normal stopping position. MIG-39 promoted the deceleration of DTCs, leading to the proper timing and positioning of the cessation of DTC migration. Among three Rac GTPase genes, mutations in *ced-10* and *rac-2* enhanced the overshoot of anterior DTCs, while they suppressed that of posterior DTCs of *mig-39* mutants. On the other hand, the mutation in *mig-2* suppressed both the anterior and posterior DTC defects of *mig-39*. Genetic analyses suggested that MIG-39 acts in parallel with Rac GTPases in stopping DTC migration. We propose a model in which the anterior and posterior DTCs respond in an opposite manner to the levels of Rac activities in the cessation of DTC migration.

Introduction

Organogenesis resulting from the budding, outgrowth and bifurcation of epithelial tubes is one of the fundamental processes of animal development. During epithelial tube morphogenesis, cells at the tip and those forming the sheath region migrate coordinately and divide at appropriate times to form elaborate branching structures (Lu and Werb, 2008). Cell migration is controlled by various molecular mechanisms, which involve extracellular matrix, growth factors, intracellular signaling cascades, the cytoskeleton and transcription factors.

As examples of this process, growth factor ligands such as fibroblast growth factor (FGF) act in lung morphogenesis by promoting the extension and branching of epithelial tubes (Min et al., 1998). In contrast, netrin blocks FGF signaling around the neck region of elongating tubes, thus preventing the formation of new buds (Liu et al., 2004). The extracellular matrix (ECM) proteins heparan sulfate proteoglycans mediate FGF signaling during kidney morphogenesis (Steer et al., 2004). The ECM protein laminin affects the branching process through the action of cell surface integrin receptors in the kidney (Kreidberg et al., 1996; Miner and Li, 2000). Mammary branching morphogenesis requires the activities of Rac, Rho kinase and myosin light-chain kinase to modulate the actomyosin network (Ewald et al., 2008). Transcription factors such as Sox9 also act in lung epithelial morphogenesis (Rockich et al., 2013).

The outgrowth or elongation of epithelial tubes is often directed by a cell or a group of cells at the tip of the growing tubes (Lu and Werb, 2008). The *Caenorhabditis elegans* gonad, which is made up of epithelial tubes, has such a cell, the distal tip cell (DTC), at the end of each arm of the gonad. Although the gonad arms do not branch, gonadal development in *C. elegans* offers a simple model for studying the tip cell-dependent spatial and temporal regulation of epithelial tube morphogenesis. Genetic analyses have uncovered various molecules that control the migration of the DTCs. The signaling molecules, such as UNC-6/netrin and UNC-129/TGFβ, are involved in the directional regulation of DTC migration (Colavita et al., 1998; Merz et al., 2001). The ECM proteins collagen IV and fibulin-1 are involved in the active migration of DTCs (Kawano et al., 2009; Kubota et al., 2004). Integrins also have important roles in DTC migration, probably by

* Corresponding author at: Department of Bioscience, Kwansei Gakuin University 2-1 Gakuen, Sanda, 669-1337, Japan. Fax: +81 79 565 9077.
E-mail address: nishiwaki@kwansei.ac.jp (K. Nishiwaki).

http://dx.doi.org/10.1016/j.ydbio.2014.10.008
0012-1606/

linking ECM and cytoskeletal activities (Meighan and Schwarzbauer, 2007). The Rho family of GTPases is involved as well in the regulation of DTC migration (Lundquist et al., 2001).

The proper timing of the cessation of tip cell migration and the correct position in the organism at which point the tip cell stops migrating are critical for producing an organ of the proper architecture and size. Although the molecular mechanisms that function in bud initiation, directional elongation and branching of epithelial tubes have been extensively studied, the mechanisms by which these tubes stop growing, for the most part, remain to be discovered.

To understand the molecular mechanisms that operate in this process, we isolated and molecularly analyzed the mutants that affect cessation of DTC migration in *C. elegans*. The causative gene for these mutations, *mig-39*, was found to encode a protein with a BED (BEAF and DREF; boundary element-associated factor and DNA replication–related element binding factor, respectively)-finger domain. The BED finger is an evolutionarily conserved Zinc-finger domain that potentially binds DNA (Aravind, 2000). Analysis of *mig-39* mutant phenotypes suggested that it is required for the deceleration of migrating DTCs to achieve their correct timing and positions for cessation. MIG-39 was expressed in the nucleus of DTCs and in the cytoplasm of germline cells. Genetic analyses suggested that MIG-39 acts in parallel with the Rac GTPase pathway in stopping DTC migration.

Materials and methods

Strains and culture conditions

Culture and handling of *C. elegans* were as described (Brenner, 1974). The following strains were used: N2 (wild type, WT), *unc-73* (*e936*), *mig-2*(*mu28*), *ced-10*(*n1993*), *rac-2*(*ok326*), *mig-39*(*tk102*, *tk107*) (this work), *dpy-18*(*e326*) *unc-69*(*e246*)*III*, *sDf110 dpy-18 (e364)/eT1III; unc-46(e177)/eT1 V, nDf16/qC1 dpy-19(e1259) glp-1 (q339)III, nDf20/sma-2(e502) unc-32(e189)III* and *nDf40 dpy-18 (e364)III; ctDp6(III; f). tkIs11 [mig-24p::venus, unc-119*(+)*]X* was generated by γ-irradiation of *unc-119*(*e2498*); *Ex[mig-24p*::*venus, unc-119*(+)*]*, a transgenic line generated by injecting 30 ng/μl *mig-24p*::*venus*, 30 ng/μl *unc-119* (+) and 140 ng/μl pBSIIKS(-) plasmids.

1.1. Isolation of the mig-39(tk102) and mig-39(tk107) mutants, genetic mapping and molecular cloning

tkIs11 [*mig-24p*::*venus, unc-119*(+)] hermaphrodites were mutagenized with ethyl methane sulfonate as described (Brenner, 1974). F2 or later young adult animals with DTCs overshot the normal positions were screened under the dissecting microscope equipped with fluorescence optics. *tk102* and *tk107* mutants were generated by ethyl methane sulfonate mutagenesis. The mutant was outcrossed eight times against the WT N2 strain. *tk102* and *tk107* were mapped to linkage group III by Sequence-Tagged Site mapping (Williams et al., 1992). Single-nucleotide polymorphism mapping combined with deletion mapping placed *tk102* and *tk107* in the regions from −0.58 to −0.19 and from −0.26 to −0.07 map units on linkage group III, respectively (Wicks et al., 2001). *tk102* and *tk107* failed to complement each other. Whole-genome sequencing revealed that the predicted gene *F42H10.5* is the sole gene in the mapped region that had mutations in both the *tk102* and *tk107* mutant genomes. Microinjection of the fosmid clone WRM0623bC05, which contains *F42H10.5*, rescued the overshoot phenotype of *tk107*. WRM0623bC05 also contained three small genes, *rpn-3* (*C30C11.2*) and *mrpl-32* (*C30C11.1*), upstream of and *F42H10.6*, downstream of *F42H10.5* (Fig. 2A). The PCR-amplified fragments containing these genes did not rescue *tk107*. Thus we concluded that *mig-39* corresponds to *F42H10.5*.

Double-stranded RNA interference (RNAi) experiments

RNAi feeding was performed as described (Fraser et al., 2000). The RNAi clone containing full-length *cacn-1* cDNA was used (Tannoury et al., 2010). The RNAi clone for *rac-2* was from the Ahringer Library (Fraser et al., 2000). The RNAi clone for *mig-2* was constructed as follows. A DNA fragment of *mig-2* containing the first and second exons was amplified from the WT genome using primers 5′-GGAA-GATCTGCAGATCAAATGTGTAGTTG-3′ and 5′-CGGGGTACCTGTTGCA-CACATTGAACCTCT-3′. The fragment was digested with KpnI and Bgl II and cloned into the RNAi vector L4440 (Grishok et al., 2005).

Analysis of DTC positions

Two transgenic makers, *tkIs11* [*mig-24p*::*venus*, *unc-119*(+)] for DTCs and *evIs82a* [*unc-129*::*gfp*] for DA and DB motor neurons (Lim and Wadsworth, 2002), were used, except that only *evIs82a* was used in the strains having *mig-2*(*mu28*). The positions of DTCs were determined relative to those of the cell bodies of the DA and DB neurons. The positions of DA and DB neurons relative to those of the vulva and gonad were not affected in the mutants other than *unc-73*. When the effect of an *unc-73* mutation was analyzed, the degree of overshoot was determined by measuring the distance from the vulva to the DTC, because *unc-73*(*e936*) showed mispositioning of DA and DB motor neurons (data not shown). The WT and mutant animals examined in this work had DTC phenotypes that were classified based on one or more of the following criteria: extra turn, wandering, premature termination and overshoot. The percentages of these phenotypes are shown in Tables S1, S2 and S3. We analyzed only the overshoot and premature termination phenotypes in the Phase III migration, because we focused on the mechanism by which DTCs stop migrating after making two normal turns.

Plasmid construction

We amplified a *mig-39* cDNA from the start to stop codons by reverse transcription of total RNA from WT animals with primers 5′-ATGAGCAGCGTAAGCAGTGATATTGATGG-3′ and 5′-CTAATTAAAAAGTTTCGAAACAATCTGACG-3′. The cDNA fragment was ligated into pGEM-T Easy Vector (Promega) (*mig-39* cDNA plasmid). To construct *lag-2p*::*mig-39* cDNA, the cloned *mig-39* cDNA region was PCR-amplified with primers 5′-ATAA-GAATGCGGCCGCGATGAGCAGCG-3′ and 5′-GGGGTACCGCGTAAT-TAAAAAGTTTCG-3′, digested with NotI and KpnI and ligated to the *lag-2p* (−7388 to +3) plasmid (Tamai and Nishiwaki, 2007) using the NotI and KpnI sites. To construct *pie-1*::*mig-39* cDNA, we amplified a *mig-39* cDNA from the *mig-39* cDNA plasmid with primers 5′- CCGCGGGAATTCGATCTAATTAAAAGTT-3′ and 5′- CAC-CATGAGCAGCGTAAGCAGTGATAT-3′. The cDNA fragment was ligated into pENTR™ Vector by Directional TOPO® Cloning Kit (Invitrogen). We used Gateway Cloning Kit (Invitrogen) to insert the *mig-39* cDNA into the MTC1G plasmid having a *pie-1* promoter (kindly provided by A. Sugimoto) and removed the *gfp* fragment by AscI digestion followed by self-ligation.

Production of transgenic animals

We injected DNA mixtures into the gonads of *mig-39*(*tk107*) adult hermaphrodites. The fosmid clone WRM0623bC05 was injected at 10 ng/μl with 30 ng/μl *myo-3*::*mCherry* marker and 110 ng/μl pBSII KS(−) plasmids. The *lag-2p*::*mig-39* cDNA plasmid was injected at 2 or 10 ng/μl with 30 ng/μl *myo-3*::*mCherry* and and pBSII KS(−) to bring total concentration to 150 ng/μl. The *pie-1p*::*mig-39* cDNA plasmid was injected at 2 ng/μl with 30 ng/μl *myo-3*::*mCherry* and 118 ng/μl pBSII KS(−). The 17-kb *mig-39* genomic fragment

encompassing from −9579 to +2770 relative to the adenine of the initiation codon was amplified by nested PCR using the external primer set 5′–GTGGGTAGGCACGATTTAAAGTGCCTGCC-3′ and 5′–CCAATAAAGTAAAGTGACAAAAGAAAAGCG-3′ and the internal primer set 5′–GGAGTCCGCATAGTATAGTTTTGCTAGC-3′ and 5′–GAGCAAC-GAGTACGACAGCTGACGTGC-3′. The fragment was injected at 2 ng/μl with 30 ng/μl *myo-3*::*mCherry* and 118 ng/μl pBSII KS(−) plasmids.

Production of antibodies

The region coding for MIG-39 peptide from M303 to H470 was amplified using primers 5′–CCGCTCGAGATGGATCTGAGCATGAAGAAG-3′ and 5′-CGGGATCCCTAATGACTTGTCGAGTTCAC-3′, digested with XhoI and BamHI and ligated into the pET-19b vector using the XhoI and BamHI sites. The antigenic peptide of MIG-39 was expressed as a histidine-tagged fusion protein in *Escherichia coli* and was used to immunize rabbits. The generated antibody was affinity purified.

Immunohistochemistry

We dissected worms on a glass slide coated with poly-L-lysine using an injection needle (Terumo 23G × $1_{1/4}$) to extrude the gonads. The samples were outlined with Dako Pen (Dako), covered with Parafilm and dried briefly. After removal of the Parafilm, the

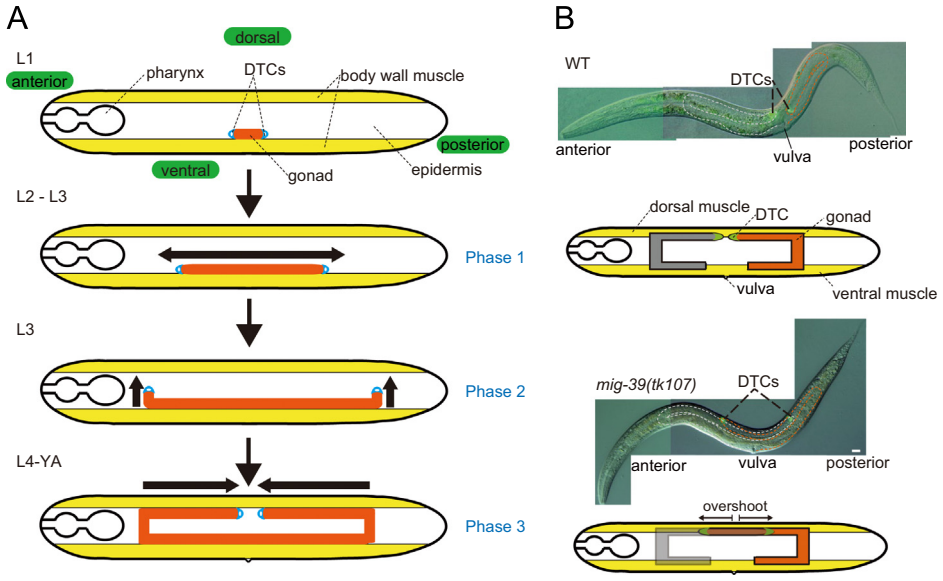

Fig. 1. DTC migration and DTC overshoot phenotype. (A) Schematic representation of the phases of DTC migration and gonad formation in the *C. elegans* hermaphrodite. (B) Merged images from Nomarski and fluorescence microscopy of WT and *mig-39*(*tk107*) hermaphrodites with a *tkIs11*[*mig-24p*::*venus*] marker. The anterior and posterior gonad arms are shown by white and red dashed outlines, respectively. The gonad shapes are schematically shown below. Scale bar: 20 μm.

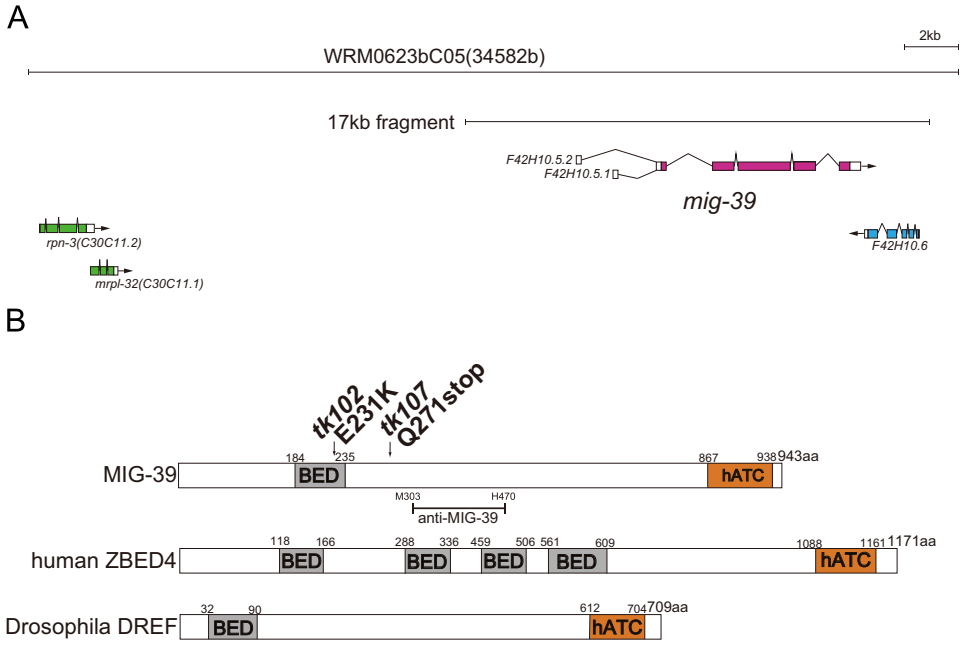

Fig. 2. Structures of the *mig-39* gene and the predicted MIG-39 protein. (A) The fosmid clone WRM0623bC05. The fosmid clone contains four protein coding genes involving *mig-39*. The protein coding regions and untranslated regions are indicated with colored and white boxes, respectively. The arrows indicate transcriptional direction. (B) Domain structures of MIG-39 and other BED-finger proteins. Positions of BED and hATC domains of MIG-39, human ZBED4 and *Drosophila* DREF are shown. Mutation sites of *tk102* and *tk107* and the region of MIG-39 used as the antigen for producing the polyclonal antibody are indicated.

samples were fixed with methanol followed by acetone for 20 min each at −20 °C and were blocked with 3.8% Block Ace (DS Pharma Biomedical Co., Ltd.) in phosphate-buffered saline (PBS). The samples were incubated with the primary antibody, anti–MIG-39, at 11.5 μg/ml in PBS containing 3.8% Block Ace for 2 h and then were incubated with the secondary antibody, Cy3-labeled anti-rabbit IgG (1:500; Life Technologies) or FITC-labeled anti-rabbit IgG (1:500; Life Technologies), and 1 μg/ml DAPI at room temperature for 40 min. The whole mount freeze fractured samples were prepared as described (Yamaguchi et al., 1983) and stained as in above.

Results

MIG-39 encodes a BED-finger protein that is required for stopping gonadal leader cell migration

The migration of the anterior and posterior gonadal leader cells, the DTCs, promotes directional elongation of gonad arms during hermaphrodite development and leads to the formation of a pair of U-shaped gonad arms with rotational symmetry. The migration of DTCs is classified into three phases (Hedgecock et al., 1987; Kimble and White, 1981). The DTCs are generated at the center of the ventral body wall muscle and migrate in opposite directions (Phase I). They turn orthogonally and migrate toward the dorsal muscle (Phase II). After reaching the dorsal muscle, the two DTCs turn again and migrate toward the mid-body (Phase III; Fig. 1(A)). We expressed Venus, a yellow fluorescent protein, under the control of the DTC-specific *mig-24* promoter and fluorescently labeled DTCs. In the WT worms, both DTCs stopped near the vulva. We isolated two mutants, *tk102* and *tk107*, whose DTCs overshot the vulval region because of a defect in the cessation of their migration (Fig. 1(B) and data not shown). Genetic analysis and molecular cloning experiments revealed that both of these mutations were recessive and were alleles of the same gene, *mig-39* (data not shown and see Materials and methods). *mig-39* corresponds to the predicted gene *F42H10.5* in WormBase, which encodes a protein with a Zinc-finger DNA-binding domain called a BED (Boundary element-associated factor and DNA replication-related element binding factor)-finger domain (Aravind, 2000). MIG-39 also has a hATC (hobo, Activator and Tam3 carboxyl-terminal) domain, which is required for self-association (Yamashita et al., 2007) (Fig. 2(B)). MIG-39 has weak homology with mammalian ZBED4 in its carboxyl terminus, which contains the hATC domain (Fig. S1). Sequencing indicated that the *tk102* and *tk107* mutations are missense (E231K) and nonsense (Q271Stop) mutations, respectively.

MIG-39 is required for deceleration of DTCs during Phase III migration

The DTC overshoot could result from a defect in body length, a defective rate of DTC migration or defective timing of the cessation of DTC migration. We compared the lengths of the bodies of WT and mutant young adult hermaphrodites and found no difference in body lengths (Fig. S2). We then examined the timing of DTC turns relative to the stages of vulval development. The vulval precursor cell P6.p undergoes three rounds of divisions and produces eight descendants, which constitute the vulval epithelium. In both WT and mutant animals, the first DTC turn occurred mostly during the four-P6.p cell stage, and the second turn occurred during the four-P6.p cell stage in ~60% of animals and during the eight-P6.p cell stage in ~40% of animals, suggesting that the migration rates in mutant DTCs until the second turn are not affected (Fig. S3). Therefore, we examined the migration during Phase III after the second turn. To quantify the DTC overshoot phenotype, we introduced an *unc-129*::*GFP* reporter, which is expressed in the DA and DB motor neurons in the ventral nerve cord. The cell bodies of these neurons were used as the longitudinal positional markers to assess the position at which DTCs ceased to migrate. The DTCs of the posterior gonad (posterior DTCs) showed stronger overshoot phenotypes than did those in the anterior gonad (anterior DTCs) in both *tk102* and *tk107* mutants (Fig. 3). We analyzed the positions of DTCs relative to

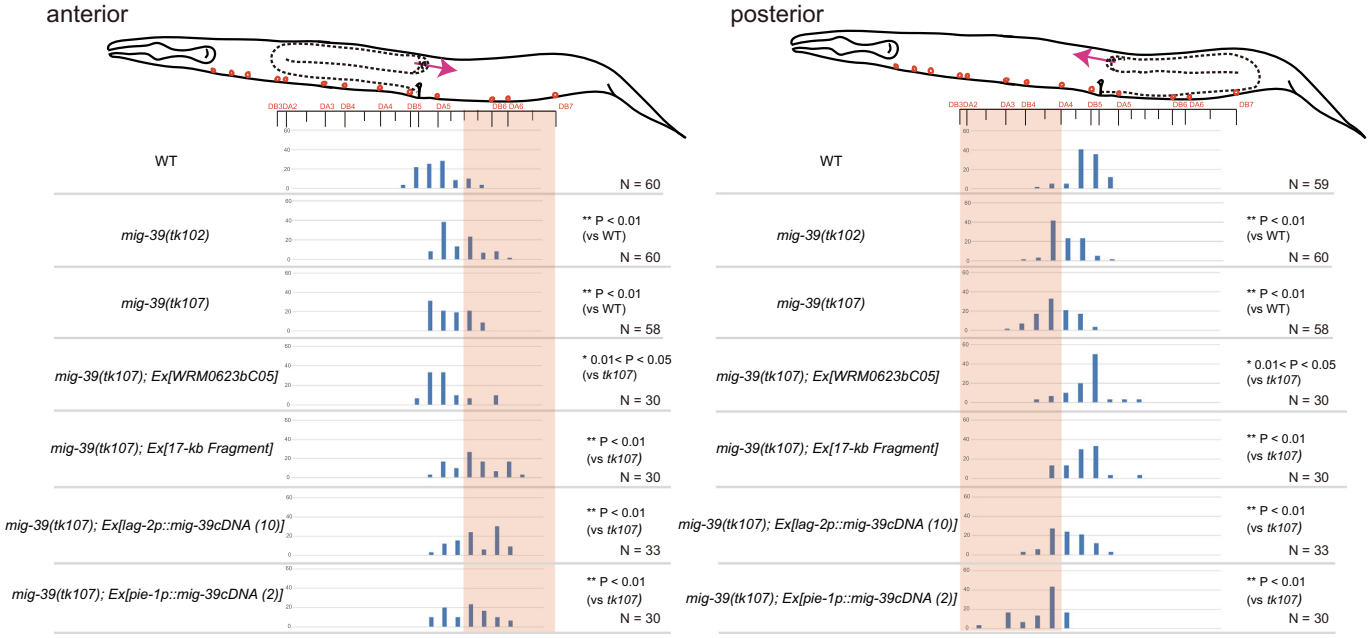

Fig. 3. Phenotypes of *mig-39* mutants and transgenics. Positions of anterior and posterior DTCs in the young adult hermaphrodites were plotted relative to the DA and DB motor neurons and the vulva. The intervals between DA2 and DA3, DB4 and DA4, DA4 and DB5 and DA6 and DB7 were each divided in half. The interval between DA5 and DB6 was divided into four equal regions. The percentages of DTCs observed in the indicated regions is shown by bar graphs. DTCs positioned in the shaded area were considered to have overshot. The *mig-39* cDNA concentrations used for microinjection are shown in the parentheses (ng/μl). More than two independent lines with similar phenotypes were obtained for WRM0623bC05, 17-kb fragment and *lag-2p*::*mig-39* cDNA transgenic lines. Of the two *pie-1p*::*mig-39* cDNA transgenic lines, one (not shown) showed enhancement of the posterior overshoot only. *P*-values for Fisher's exact test are indicated when <0.05.

those of the DA and DB neurons in time course experiments during Phase III migration. Although we detected subtle differences in migration rates between WT and mutants in the anterior DTCs, clear differences were observed in the posterior DTCs (Fig. 4). In the WT, the posterior DTCs gradually decelerated after the second turn and stopped around DB5 neuron ~15 h after the second turn, when animals reached the adult stage. The DTCs retracted after that to positions near the vulva by ~24 h; this slight relative retraction could have resulted from elongation of the body. In contrast, the DTCs in *tk102* and *tk107* mutants stopped ~16 and 18 h, respectively, after the second turn, and they also retracted to some extent until 24 h. These results indicate that the migration rates of mutant DTCs are not faster than the migration rate of WT DTCs during Phase III, but rather that the deceleration rates were slower in the mutants compared with the WT, and therefore the mutant DTCs stopped migrating later than did the WT DTCs.

MIG-39 protein is expressed in DTCs and germline cells

We generated a polyclonal antibody against a region of the MIG-39 polypeptide that was expressed in *E. coli* (Fig. 2(B)). This antibody recognized nuclear antigens of DTCs as well as antigens in the cytoplasm of germline cells in WT animals (Fig. 5(A) and (B)). Although it also stained the same tissues in the *tk102* mutant, it failed to stain those of the *tk107* mutant animals. Thus it is likely that the antibody specifically recognized the MIG-39 protein and that *tk107* is a null allele. To examine the localization of MIG-39 in the nucleus, we stained the gonads of the animals expressing UNC-84-GFP. UNC-84 is the *C. elegans* homolog of the SUN protein, which localizes to the inner nuclear membrane (Malone et al., 1999). MIG-39 preferentially localized to the peripheral chromatin region of the nucleus of DTCs (Fig. 5(C)). We then examined the expression of MIG-39 in the WT DTCs in time course experiments. We observed that the expression of MIG-39 in the DTC nucleus progressively decreased across fourth larval stage (L4), young adult and late adult animals (Fig. 5(D)).

Transgenic rescue of mig-39 mutants

The fosmid clone WRM0623bC05 fully rescued the cessation defect of DTCs in *mig-39*(*tk107*) mutants (Fig. 3). However, when we used a 17-kb PCR-amplified fragment of *mig-39* with a 9579-bp 5′ untranslated region, it enhanced the anterior defect although the posterior defect was suppressed (Fig. 3). These results suggested that the 17-kb fragment may lack sequences required for proper regulation of *mig-39* expression. Because MIG-39 is expressed in DTCs and germline cells, we expected that MIG-39 could act in the

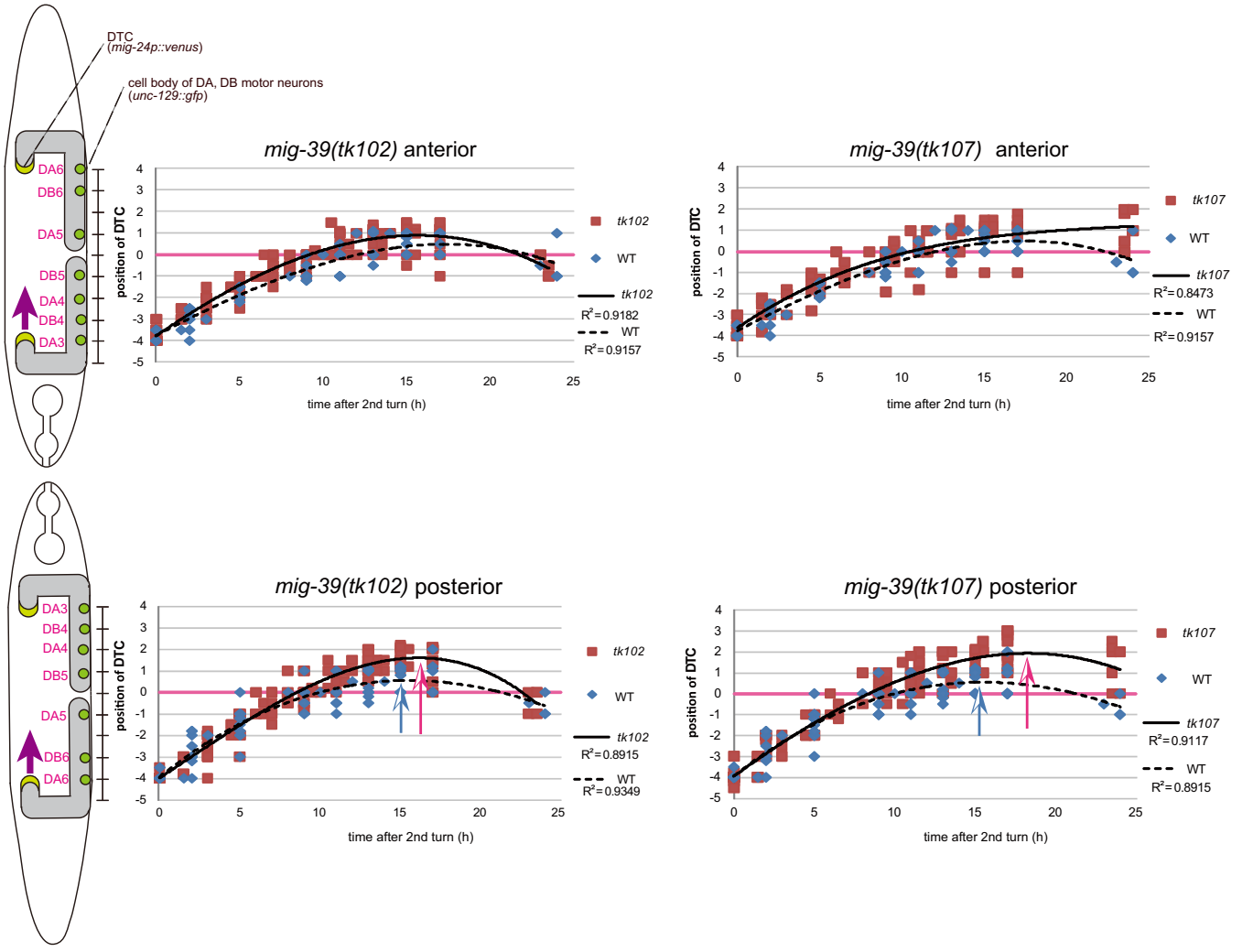

Fig. 4. Analysis of Phase III migration. Positions of DTCs relative to those of the DA and DB neurons in the time course experiments during Phase III migration were plotted. The *x* axis represents the time after the second turn, and the *y* axis represents the position of each DTC, with the position of the developing vulva considered as zero. Each red square (WT) and blue rhombus (mutant) represents a single DTC. The curves were drawn using Excel (Microsoft) based on third-degree polynomial approximation. R^2 values are indicated. In the posterior DTCs, arrows indicate their peak positions.

DTCs themselves. We expressed the *mig-39* cDNA in DTCs using the DTC-specific *lag-2* promoter and observed that the transgenic animals exhibited suppression of the posterior phenotype, whereas the anterior phenotype was enhanced, as was the case for the 17-kb fragment (Fig. 3). Thus DTC-specific expression of MIG-39 was sufficient for the posterior DTC to stop appropriately but was not sufficient for the regulation of anterior DTC stopping. Alternatively, the anterior and posterior DTCs may respond differently to overproduction of MIG-39. Supporting for this, we observed that overproduction of MIG-39 in the wild type background resulted in anterior overshoot (Fig S4). We then expressed *mig-39* cDNA under the germline-specific *pie-1* promoter. We observed no suppression of the *mig-39* phenotype and rather enhancement of the anterior and posterior overshoot, indicating that germline expression of MIG-39 cannot rescue the *mig-39* defects (Fig. 3).

CACN-1 acts in parallel with MIG-39

RNAi of CACN-1, the *C. elegans* homolog of *Drosophila* Cactin, causes DTC overshooting (Tannoury et al., 2010). We thus examined the genetic interaction between CACN-1 and MIG-39. *cacn-1* RNAi showed a weak overshoot phenotype of the posterior DTCs. This could be because of that *cacn-1* RNAi treated DTCs continue to migrate after the young adult stage at which we scored the

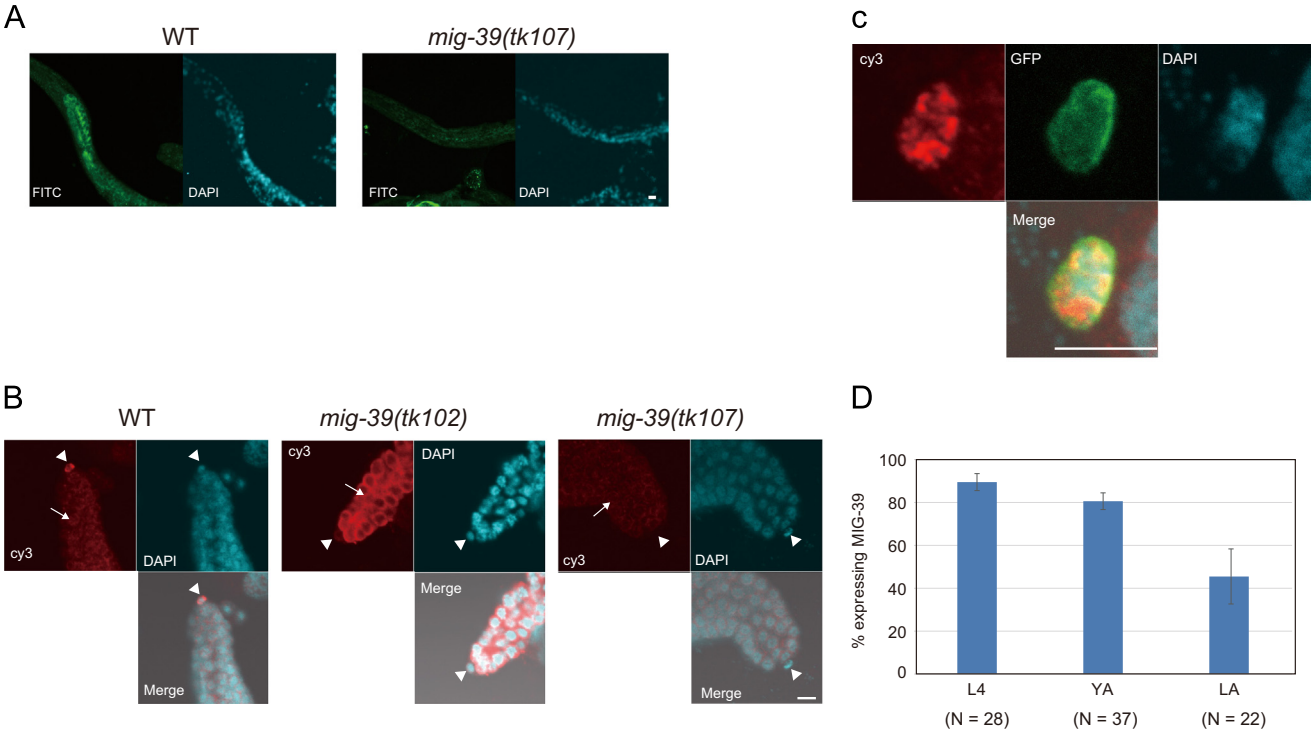

Fig. 5. Expression of MIG-39. (A) Whole mount freeze fractured specimens of wild type and *mig-39* mutant L4 hermaphrodites stained with ani-MIG-39 (green) and DAPI (blue). FITC-labeled anti-rabbit IgG was used as the secondary antibody. The germline tissue is stained in the wild type, but not in the mutant animals. The DTCs cannot be identified in these photos. Scale bar: 10 μm. (B) Immunostaining of dissected gonads using anti-MIG-39. Cy3-labeled anti–rabbit IgG was used as the secondary antibody. Cy3, DAPI and the merged images of young adult stage WT (left), *mig-39*(*tk102*) (middle) and *mig-39*(*tk107*) (right) animals are shown. Arrows and arrowheads indicate germline and DTCs, respectively. Scale bar: 10 μm. (C) A WT DTC expressing UNC-84-GFP stained with anti-MIG-39 (red), anti-GFP (green) and DAPI (blue). Merged image is shown below. Scale bar: 10 μm. (D) Percentages of MIG-39-expressing DTCs in L4, young adult (YA) and 2-day adult (LA) WT animals. Data are shown as the mean ± standard deviation. N, number of DTCs examined.

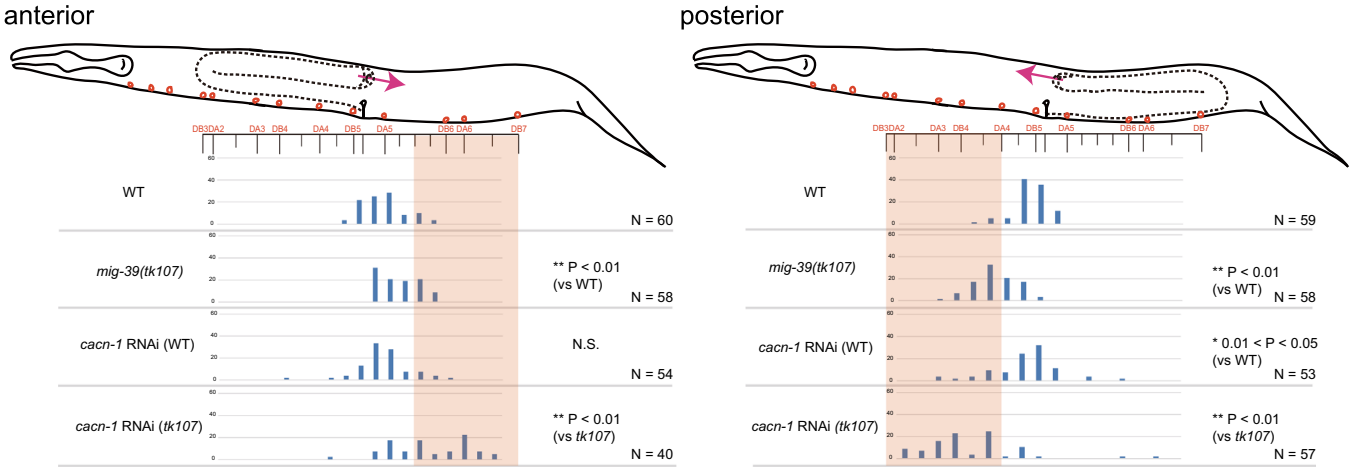

Fig. 6. Enhancement of *mig-39* phenotypes by *cacn-1* RNAi. DTC positions were scored as in Fig. 3. N.S., not significant. P-values for Fisher's exact test are indicated when < 0.05.

phenotype (Tannoury et al., 2010). When we conducted *cacn-1* RNAi in the *mig-39*(*tk107*) background, we observed significant enhancement of the overshoot phenotype for both anterior and posterior DTCs. We used the *tk107* allele rather than *tk102* because it is likely to be a null allele. These results suggest that *cacn-1* acts in parallel with *mig-39* for DTC cessation (Fig. 6).

Rac GTPases act in parallel pathways relative to MIG-39

Rac GTPases play important roles in cell migration and axon extension by regulating the actin cytoskeleton (Burridge and Wennerberg, 2004). Among three Rac proteins in *C. elegans*, CED-10 and MIG-2 have been implicated in the regulation of DTC migration (Cabello et al., 2010; Lundquist et al., 2001; Peters et al., 2013; Reddien and Horvitz, 2000). In particular, MIG-2 is suggested to interact with CACN-1 to stop DTC migration (Tannoury et al., 2010). So far, there has been no description of the activity of the third Rac protein, RAC-2, in DTC migration.

We examined the effects of Rac GTPases and one of their GTP exchange factors, UNC-73 (Wu et al., 2002), on the cessation of DTC migration. We used null mutations *rac-2(ok326)* and *mig-2 (mu28)* and reduced-function mutations *ced-10(n1993)* and *unc-73 (e936)*. No overshoot phenotype was detected in *ced-10(n1993)* and *mig-2(mu28)* single mutants. *rac-2(ok326)* showed overshoot of the anterior DTCs, and *unc-73(e936)* did for both anterior and posterior DTCs. When combined with *mig-39(tk107)*, *ced-10* and *rac-2* enhanced the anterior defect, whereas they suppressed the posterior defect of this *mig-39* mutant. In contrast, *mig-2* suppressed both anterior and posterior defects, and *unc-73* did not affect the anterior overshoot of *mig-39* but did strongly enhance its posterior overshoot defect (Fig. 7(A) and (B)).

Because the three Rac genes act in a redundant manner in the migration of various cells and axons (Kishore and Sundaram, 2002; Shakir et al., 2006; Wu et al., 2002), we conducted double knockdown of Rac genes using RNAi. We found that *rac-2* RNAi in *ced-10 (n1993); mig-39(tk107)* and *rac-2* RNAi in *mig-2(mu28)*; *mig-39 (tk107)* animals suppressed the *mig-39(tk107)* overshoot defects for both anterior and posterior DTCs and that *mig-2* RNAi in *ced-10 (n1993); mig-39(tk107)* animals suppressed the posterior overshoot of *mig-39* (Fig. 7(A)). These data indicated that the requirements of Rac activities for stopping DTC migration differ between the anterior and posterior DTCs.

Discussion

MIG-39 is specifically required for the cessation of DTC migration

In the present study, we identified *mig-39*, a gene that is required for proper deceleration of DTCs, through forward genetics analysis. Two genes have been reported to affect the cessation of DTC migration: *cacn-1* and *ccdc-55*. CACN-1 is the homolog of the *Drosophila* Cactin, which is required for the formation of embryonic dorso-ventral polarity (Tannoury et al., 2010). CACN-1 was recently shown to be a component of the splicesome in *C. elegans* (Doherty et al., 2014). CCDC-55 is a coiled-coil domain protein that is conserved throughout eukaryotes (Kovacevic et al., 2012). Deletion mutations of these genes result in larval arrest, but the DTC overshoot phenotypes can be observed using RNAi knockdown (Kovacevic et al., 2012; Tannoury et al., 2010). Therefore, these genes appear to be required for larval growth as well as for the cessation of DTC migration. In contrast to these genes, *mig-39* is required specifically for the stopping of DTCs because we detected no other phenotypes in the *tk107* null mutant. Because in our screen we obtained only two independent mutants that affect the cessation of DTC migration, which were both shown to be alleles of *mig-39*, it is possible that the number of genes functioning specifically in DTC stopping could be relatively small.

Expression and function of MIG-39

The BED-finger domain-containing proteins are evolutionarily conserved DNA-binding proteins that are implicated in the regulation of chromatin structure, DNA replication and transcription (Aravind, 2000). BEAF was originally identified as a protein that localizes to interbands and puff boundaries on polytene chromosomes in *Drosophila* (Zhao et al., 1995). BEAF is an insulator protein predominantly found near gene promoters and has a role in the expression of genes involved in cell cycle regulation, chromosome segregation and cell polarity (Emberly et al., 2008; Gurudatta et al., 2012). DREF in *Drosophila* (Hirose et al., 1996) forms a multisubunit protein complex with TATA box-binding protein (TBP)-related factor 2 (TRF2) (Hochheimer et al., 2002) and acts as a transcription factor for S-phase genes such as those that encode PCNA, DNA polymerase α, Cyclin A, D-raf and Warts (Fujiwara et al., 2012; Hirose et al., 1993; Ohno et al., 1996; Ryu et al., 1997). DREF is suggested to be involved in cell proliferation by antagonizing the action of BEAF (Emberly et al., 2008; Hart et al., 1999). The human homolog of DREF is also involved in cell proliferation and the expression of histone H1 and ribosomal genes (Ohshima et al., 2003; Yamashita et al., 2007).

In the present work, we first demonstrated the function of this BED-finger protein in cell migration, especially in the regulation of cessation of cell migration. We found that MIG-39 localized to the DTC nucleus, whereas it was found in the cytoplasm of germline cells. Although MIG-39 acted cell-autonomously (at least for posterior DTCs) in stopping migration, its function in the germline is not clear. Nuclear and cytoplasmic localization of BED-finger proteins occurs in other systems: *Drosophila* DREF is expressed in both the nucleus and cytoplasm in early embryos (Hirose et al., 1996), and human ZBED4 localizes to both the nucleus of retinal cone photoreceptors and the cytoplasm of their pedicles and inner segments. It is also expressed in the endfeet of glial Muller cells but not in their nuclei (Saghizadeh et al., 2009). No function has been implicated for these proteins when expressed in the cytoplasm.

MIG-39 and Rac functions in the cessation of DTC migration

Among the Rac mutants, only *rac-2* and *ced-10* showed overshoot of the anterior DTCs. These mutants, when combined with the *mig-39(tk107)* null allele, enhanced the anterior overshoot phenotype of *mig-39*, suggesting that *rac-2* and *ced-10* act in parallel with *mig-39*. Because *mig-2* suppressed both anterior and posterior overshoot of *mig-39*, it is not clear whether *mig-2* acts in parallel with or downstream of *mig-39*. However, given the functional redundancy of Racs in DTC migration, it is possible that *mig-2* also acts in parallel with *mig-39*. We examined the expression of *mig-2* fused with *gfp* in DTCs in *mig-39* and control RNAi experiments and observed no difference in the levels of GFP expression, suggesting that *mig-2* is not a transcriptional target downstream of MIG-39 (data not shown). Because all the Rac mutants exhibited enhancing or suppressing effects on the overshoot phenotypes of *mig-39*, it is possible that the functions of Racs become apparent when placed in the *mig-39* mutant background.

To interpret the actions of Racs that we observed in the *mig-39* background, we postulated that (1) the three Racs act redundantly in the regulation of DTC stopping, (2) the effect of *mig-2* on DTC stopping is larger than that of *ced-10* or *rac-2* and (3) the sum total of Rac activity is most severely reduced in the *unc-73* mutant. Based on these hypotheses, we can infer the levels of Rac activities

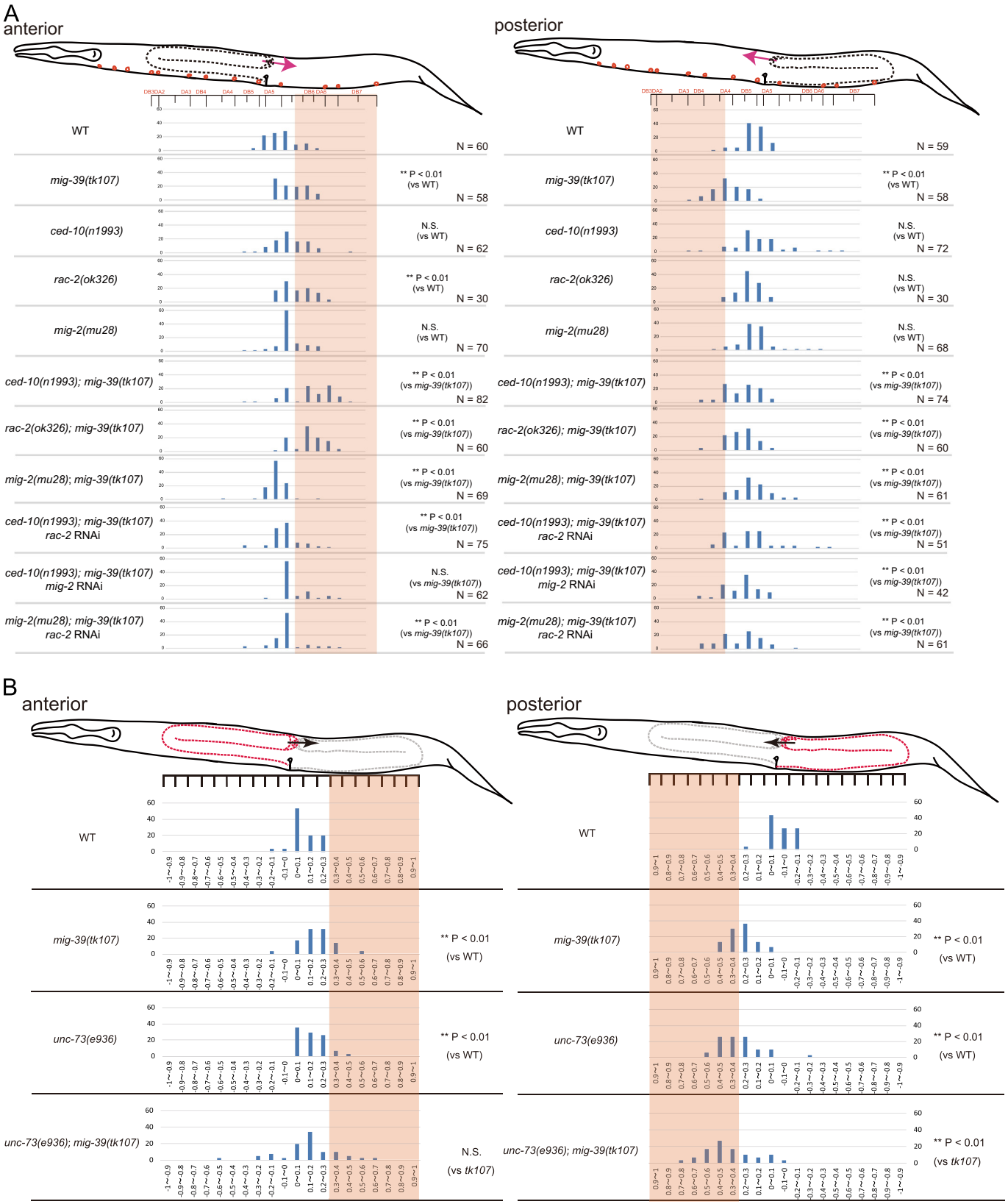

Fig. 7. Genetic interaction between *mig-39* and Rac or GTP exchange factor mutants. (A) DTC positions were scored as in Fig. 3. *P*-values for Fisher's exact test are indicated when <0.05. N.S., not significant. Some RNAi cross-silencing might be considered because of the DNA sequence similarities among Racs although the similarities are low. (B) The positions of DTCs were determined by measuring their distance from the vulva. The distance from the vulva to the gonadal loop region was divided into ten equal regions for anterior and posterior gonads, and the percentages of DTCs mapped to the regions were shown by bar graphs. DTCs positioned in the shaded area were considered to have overshot. *P*-values for Fisher's exact test are indicated when <0.05. N.S., not significant.

in each strain as shown in Fig. 8. If this is the case, it is possible that as for the anterior DTCs, the reduction of Rac activity to certain levels promotes DTC overshoot and therefore enhances *mig-39*, whereas further reduction promotes DTC stopping and therefore suppresses *mig-39* (Fig. 8(A)). In contrast, the posterior DTCs may respond to the Rac levels in an opposite manner: the reduction to certain levels causes promotion of DTC stopping, whereas further reduction results in promotion of DTC overshoot (Fig. 8(B)). This model is, for the most part, consistent with our observations. Although the overshooting of the anterior DTCs in *ced-10(n1993); mig-39(tk107)* animals in the presence of *mig-2* RNAi was not significantly suppressed as compared with that in *mig-39(tk107)* animals, this phenotype was significantly less severe as compared with that in *ced-10(n1993); mig-39(tk107)* animals (Fig. 7(A)). Although the overshooting of the anterior DTCs in *unc-73(e936)*; *mig-39(tk107)* animals was not significantly suppressed as compared with that in *mig-39(tk107)* animals, the premature termination phenotype was enhanced: 3% in *mig-39 (tk107)* compared with 17% in *unc-73(e936); mig-39(tk107)* when considering premature stopping positions < -0.1 (Fig. 7(B)).

We have previously observed similar opposite responses in anterior and posterior DTCs when we combined *sqv-5*/*chondroitin synthase* or *mig-22*/*chondroitin polymerizing factor* mutants with mutations in *unc-6*/*netrin* or its receptors *unc-5* and *unc-40* (Suzuki et al., 2006). Mutations in *unc-6*, *unc-5* or *unc-40* all enhanced the dorsal migration defect of the posterior DTCs, but concomitantly they suppressed the defect of the anterior DTCs of *sqv-5* and *mig-22* mutants. We proposed a model that the UNC-6/netrin guidance signal could be bidirectional and that the balance between repulsive and attractive activities determines the direction of DTC migration. The anterior and posterior DTCs may have different settings for the balance points in response to the levels of UNC-6 signal. The Phase III migration of DTCs might be regulated similarly by the balance between bidirectional activities that are generated by Rac GTPases, which leads the DTCs to stop migrating when these activities become proportional. Because the two DTCs normally migrate in opposite directions in the Phase III migration, it is also possible that they have opposite settings for responding to Rac levels during this migratory phase. It has been reported that Semaphorin-1 and Plexin-1 signaling, which is normally attractive, becomes repulsive when Rac levels are reduced in the positioning of male ray 1 precursor cells (Dalpé et al., 2004). Because the DTC overshoot phenotype is stronger in the posterior DTCs as compared with the anterior DTCs in *mig-39* mutants and because the overproduction of MIG-39 suppresses the posterior phenotype and enhances the anterior phenotype of *mig-39*, it is also possible that anterior and posterior DTCs have different settings for responding to the levels of MIG-39 activity.

When considering the mechanism of DTC migration, we should bear in mind that the anterior and posterior DTCs migrate in different fields: although the anterior and posterior DTCs migrate in a similar U-shaped pattern, they migrate over the anterior and posterior body wall, respectively. During Phase III migration, the DTC at the tip of the anterior gonad migrates toward the tail,

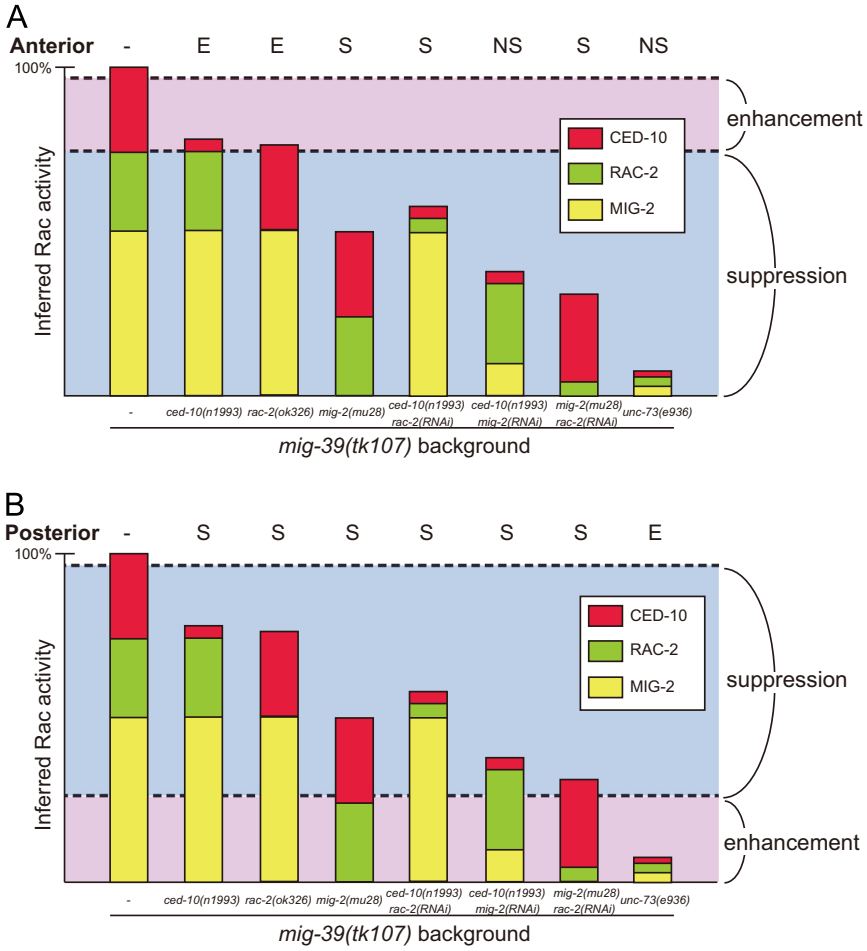

Fig. 8. Model for Rac activity-dependent responses of DTC overshoot in *mig-39* mutants. Expected levels of Rac activity in each genotype are shown in the bar graphs. The Racs may be partially redundant because there are effectors other than UNC-73. The ranges of Rac activities proposed to enhance the overshoot phenotype of *mig-39* are shown in pink, and those proposed to suppress it are shown in blue for anterior (A) and posterior (B) DTCs. The observed outcomes are indicated: E, enhancement; S, suppression; NS, not significant.

whereas that of the posterior gonad migrates toward the head along the dorsal body wall muscle. There are secreted signaling molecules distributed in a gradient along the antero-posterior axis of the developing animal. For example, EGL-20/Wnt is expressed in muscle and epidermal cells in the tail region and is distributed in a posterior-to-anterior gradient (Coudreuse et al., 2006). Thus it is possible that the two DTCs sense opposite gradients of such signaling molecules. It would be interesting to examine whether secreted signaling molecules act to stop DTC migration and whether MIG-39 is affected at its level of expression, activity or localization by such signals to regulate the cessation of DTC migration.

Acknowledgments

We thank Erin J. Cram for the *cacn-1* RNAi clone, Asako Sugimoto for the MTC1G plasmid. Some nematode strains used in this work were provided by the Caenorhabditis Genetics Center, which is funded by the NIH National Center for Research Resources (NCRR). This work was supported by a Grant-in-aid for scientific research on innovative areas by the Ministry of Education, Culture, Sports, Science and Technology to KN (22111005).

Appendix A. Supplementary information

Supplementary data associated with this article can be found in the online version at http://dx.doi.org/10.1016/j.ydbio.2014.10.008.

References

Aravind, L., 2000. The BED finger, a novel DNA-binding domain in chromatin-boundary-element-binding proteins and transposases. Trends Biochem. Sci. 25, 421–423.
Brenner, S., 1974. The genetics of *Caenorhabditis elegans*. Genetics 77, 71–94.
Burridge, K., Wennerberg, K., 2004. Rho and Rac take center stage. Cell 116, 167–179.
Cabello, J., Neukomm, L.J., Günesdogan, U., Burkart, K., Charette, S.J., Lochnit, G., Hengartner, M.O., Schnabel, R., 2010. The Wnt pathway controls cell death engulfment, spindle orientation, and migration through CED-10/Rac. PLoS Biol. 8, e1000297.
Colavita, A., Krishna, S., Zheng, H., Padgett, R.W., Culotti, J.G., 1998. Pioneer axon guidance by UNC-129, a *C. elegans* TGF-beta. Science 281, 706–709.
Coudreuse, D.Y., Roël, G., Betist, M.C., Destrée, O., Korswagen, H.C., 2006. Wnt gradient formation requires retromer function in Wnt-producing cells. Science 312, 921–924.
Dalpé, G., Zhang, L.W., Zheng, H., Culotti, J.G., 2004. Conversion of cell movement responses to Semaphorin-1 and Plexin-1 from attraction to repulsion by lowered levels of specific RAC GTPases in *C. elegans*. Development 131, 2073–2088.
Doherty, M.F., Adelmant, G., Cecchetelli, A.D., Marto, J.A., Cram, E.J., 2014. Proteomic analysis reveals CACN-1 is a component of the spliceosome in *Caenorhabditis elegans*. G3 (Bethesda) 4, 1555–1564.
Emberly, E., Blattes, R., Schuettengruber, B., Hennion, M., Jiang, N., Hart, C.M., Käs, E., Cuvier, O., 2008. BEAF regulates cell-cycle genes through the controlled deposition of H3K9 methylation marks into its conserved dual-core binding sites. PLoS Biol. 6, 2896–2910.
Ewald, A.J., Brenot, A., Duong, M., Chan, B.S., Werb, Z., 2008. Collective epithelial migration and cell rearrangements drive mammary branching morphogenesis. Dev. Cell. 14, 570–581.
Fraser, A.G., Kamath, R.S., Zipperlen, P., Martinez-Campos, M., Sohrmann, M., Ahringer, J., 2000. Functional genomic analysis of *C. elegans* chromosome I by systematic RNA interference. Nature 408, 325–330.
Fujiwara, S., Ida, H., Yoshioka, Y., Yoshida, H., Yamaguchi, M., 2012. The warts gene as a novel target of the *Drosophila* DRE/DREF transcription pathway. Am. J. Cancer Res. 2, 36–44.
Grishok, A., Sinskey, J.L., Sharp, P.A., 2005. Transcriptional silencing of a transgene by RNAi in the soma of *C. elegans*. Genes Dev. 19, 683–696.
Gurudatta, B.V., Ramos, E., Corces, V.G., 2012. The BEAF insulator regulates genes involved in cell polarity and neoplastic growth. Dev. Biol. 369, 124–132.
Hart, C.M., Cuvier, O., Laemmli, U.K., 1999. Evidence for an antagonistic relationship between the boundary element-associated factor BEAF and the transcription factor DREF. Chromosoma 108, 375–383.
Hedgecock, E.M., Culotti, J.G., Hall, D.H., Stern, B.D., 1987. Genetics of cell and axon migrations in *Caenorhabditis elegans*. Development 100, 365–382.
Hirose, F., Yamaguchi, M., Handa, H., Inomata, Y., Matsukage, A., 1993. Novel 8-base pair sequence (Drosophila DNA replication-related element) and specific binding factor involved in the expression of Drosophila genes for DNA polymerase alpha and proliferating cell nuclear antigen. J. Biol. Chem. 268, 2092–2099.
Hirose, F., Yamaguchi, M., Kuroda, K., Omori, A., Hachiya, T., Ikeda, M., Nishimoto, Y., Matsukage, A., 1996. Isolation and characterization of cDNA for DREF, a promoter-activating factor for Drosophila DNA replication-related genes. J. Biol. Chem. 271, 3930–3937.
Hochheimer, A., Zhou, S., Zheng, S., Holmes, M.C., Tjian, R., 2002. TRF2 associates with DREF and directs promoter-selective gene expression in Drosophila. Nature 420, 439–445.
Kawano, T., Zheng, H., Merz, D.C., Kohara, Y., Tamai, K.K., Nishiwaki, K., Culotti, J.G., 2009. *C. elegans* mig-6 encodes papilin isoforms that affect distinct aspects of DTC migration, and interacts genetically with mig-17 and collagen IV. Development 136, 1433–1442.
Kimble, J.E., White, J.G., 1981. On the control of germ cell development in *Caenorhabditis elegans*. Dev. Biol. 81, 208–219.
Kishore, R.S., Sundaram, M.V., 2002. ced-10 Rac and mig-2 function redundantly and act with unc-73 trio to control the orientation of vulval cell divisions and migrations in Caenorhabditis elegans. Dev. Biol. 241, 339–348.
Kovacevic, I., Ho, R., Cram, E.J., 2012. CCDC-55 is required for larval development and distal tip cell migration in *Caenorhabditis elegans*. Mech. Dev. 128, 548–559.
Kreidberg, J.A., Donovan, M.J., Goldstein, S.L., Rennke, H., Shepherd, K., Jones, R.C., Jaenisch, R., 1996. Alpha 3 beta 1 integrin has a crucial role in kidney and lung organogenesis. Development 122, 3537–3547.
Kubota, Y., Kuroki, R., Nishiwaki, K., 2004. A fibulin-1 homolog interacts with an ADAM protease that controls cell migration in *C. elegans*. Curr. Biol. 14, 2011–2018.
Lim, Y.S., Wadsworth, W.G., 2002. Identification of domains of netrin UNC-6 that mediate attractive and repulsive guidance and responses from cells and growth cones. J. Neurosci. 22, 7080–7087.
Liu, Y., Stein, E., Oliver, T., Li, Y., Brunken, W.J., Koch, M., Tessier-Lavigne, M., Hogan, B.L., 2004. Novel role for Netrins in regulating epithelial behavior during lung branching morphogenesis. Curr. Biol. 14, 897–905.
Lu, P., Werb, Z., 2008. Patterning mechanisms of branched organs. Science 322, 1506–1509.
Lundquist, E.A., Reddien, P.W., Hartwieg, E., Horvitz, H.R., Bargmann, C.I., 2001. Three *C. elegans* Rac proteins and several alternative Rac regulators control axon guidance, cell migration and apoptotic cell phagocytosis. Development 128, 4475–4488.
Malone, C.J., Fixsen, W.D., Horvitz, H.R., Han, M., 1999. UNC-84 localizes to the nuclear envelope and is required for nuclear migration and anchoring during *C. elegans* development. Development 126, 3171–3181.
Meighan, C.M., Schwarzbauer, J.E., 2007. Control of *C. elegans* hermaphrodite gonad size and shape by vab-3/Pax6-mediated regulation of integrin receptors. Genes. Dev. 21, 1615–1620.
Merz, D.C., Zheng, H., Killeen, M.T., Krizus, A., Culotti, J.G., 2001. Multiple signaling mechanisms of the UNC-6/netrin receptors UNC-5 and UNC-40/DCC in vivo. Genetics 158, 1071–1080.
Min, H., Danilenko, D.M., Scully, S.A., Bolon, B., Ring, B.D., Tarpley, J.E., DeRose, M., Simonet, W.S., 1998. Fgf-10 is required for both limb and lung development and exhibits striking functional similarity to Drosophila branchless. Genes. Dev. 12, 3156–3161.
Miner, J.H., Li, C., 2000. Defective glomerulogenesis in the absence of laminin alpha5 demonstrates a developmental role for the kidney glomerular basement membrane. Dev. Biol. 217, 278–289.
Ohno, K., Hirose, F., Sakaguchi, K., Nishida, Y., Matsukage, A., 1996. Transcriptional regulation of the Drosophila CycA gene by the DNA replication-related element (DRE) and DRE binding factor (DREF). Nucl. Acids Res. 24, 3942–3946.
Ohshima, N., Takahashi, M., Hirose, F., 2003. Identification of a human homologue of the DREF transcription factor with a potential role in regulation of the histone H1 gene. J. Biol. Chem. 278, 22928–22938.
Peters, E.C., Gossett, A.J., Goldstein, B., Der, C.J., Reiner, D.J., 2013. Redundant canonical and noncanonical *Caenorhabditis elegans* p21-activated kinase signaling governs distal tip cell migrations. G3 (Bethesda) 3, 181–195.
Reddien, P.W., Horvitz, H.R., 2000. CED-2/CrkII and CED-10/Rac control phagocytosis and cell migration in *Caenorhabditis elegans*. Nat. Cell Biol. 2, 131–136.
Rockich, B.E., Hrycaj, S.M., Shih, H.P., Nagy, M.S., Ferguson, M.A., Kopp, J.L., Sander, M., Wellik, D.M., Spence, J.R., 2013. Sox9 plays multiple roles in the lung epithelium during branching morphogenesis. Proc. Natl. Acad. Sci. USA 110, E4456–4464.
Ryu, J.R., Choi, T.Y., Kwon, E.J., Lee, W.H., Nishida, Y., Hayashi, Y., Matsukage, A., Yamaguchi, M., Yoo, M.A., 1997. Transcriptional regulation of the Drosophila-raf proto-oncogene by the DNA replication-related element (DRE)/DRE-binding factor (DREF) system. Nucleic Acids Res. 25, 794–799.
Saghizadeh, M., Akhmedov, N.B., Yamashita, C.K., Gribanova, Y., Theendakara, V., Mendoza, E., Nelson, S.F., Ljubimov, A.V., Farber, D.B., 2009. ZBED4, a BED-type zinc-finger protein in the cones of the human retina. Investig. Ophthalmol Vis. Sci. 50, 3580–3588.
Shakir, M.A., Gill, J.S., Lundquist, E.A., 2006. Interactions of UNC-34 Enabled with Rac GTPases and the NIK kinase MIG-15 in *Caenorhabditis elegans* axon pathfinding and neuronal migration. Genetics 172, 893–913.
Steer, D.L., Shah, M.M., Bush, K.T., Stuart, R.O., Sampogna, R.V., Meyer, T.N., Schwesinger, C., Bai, X., Esko, J.D., Nigam, S.K., 2004. Regulation of ureteric bud branching morphogenesis by sulfated proteoglycans in the developing kidney. Dev. Biol. 272, 310–327.

Suzuki, N., Toyoda, H., Sano, M., Nishiwaki, K., 2006. Chondroitin acts in the guidance of gonadal distal tip cells in *C. elegans*. Dev. Biol. 300, 635–646.
Tamai, K.K., Nishiwaki, K., 2007. bHLH transcription factors regulate organ morphogenesis via activation of an ADAMTS protease in *C. elegans*. Dev. Biol. 308, 562–571.
Tannoury, H., Rodriguez, V., Kovacevic, I., Ibourk, M., Lee, M., Cram, E.J., 2010. CACN-1/Cactin interacts genetically with MIG-2 GTPase signaling to control distal tip cell migration in *C. elegans*. Dev. Biol. 341, 176–185.
Wicks, S.R., Yeh, R.T., Gish, W.R., Waterston, R.H., Plasterk, R.H., 2001. Rapid gene mapping in *Caenorhabditis elegans* using a high density polymorphism map. Nat. Genet. 28, 160–164.
Williams, B.D., Schrank, B., Huynh, C., Shownkeen, R., Waterston, R.H., 1992. A genetic mapping system in *Caenorhabditis elegans* based on polymorphic sequence-tagged sites. Genetics 131, 609–624.
Wu, Y.C., Cheng, T.W., Lee, M.C., Weng, N.Y., 2002. Distinct rac activation pathways control Caenorhabditis elegans cell migration and axon outgrowth. Dev. Biol. 250, 145–155.
Yamaguchi, Y., Murakami, K., Furusawa, M., Miwa, J., 1983. Germline-specific antigens identified by monoclonal antibodies in the nematode *C. elegans*. Dev. Growth Differ. 25, 121–131.
Yamashita, D., Sano, Y., Adachi, Y., Okamoto, Y., Osada, H., Takahashi, T., Yamaguchi, T., Osumi, T., Hirose, F., 2007. hDREF regulates cell proliferation and expression of ribosomal protein genes. Mol. Cell Biol. 27, 2003–2013.
Zhao, K., Hart, C.M., Laemmli, U.K., 1995. Visualization of chromosomal domains with boundary element-associated factor BEAF-32. Cell 81, 879–889.